Table 4 Diagnostic value of endoscopic features in the antrum for *H. pylori* infection

		H. pylori positive	*H. pylori* negative	Total	ROC/AUC (95% CI)	Sensitivity (%) (95% CI)	Specificity (%) (95% CI)	PPV (%) (95% CI)	NPV (%) (95% CI)
Diffuse redness	+	83	71	154	0.646	73.5	55.9	53.9	75.0
	–	30	90	120	(0.584–0.708)	(64.3–81.3)	(47.9–63.7)	(45.7–61.9)	(66.3–82.5)
Spotty redness	+	37	45	82	0.525	33.0	71.9	45.1	60.5
	–	75	115	190	(0.467–0.581)	(24.4–42.6)	(64.2–78.7)	(34.1–56.5)	(53.2–67.5)
Mucosal swelling	+	65	41	106	0.669	60.7	73.0	61.3	72.5
	–	42	111	153	(0.610–0.727)	(50.8–70.0)	(65.2–79.9)	(51.4–70.6)	(64.8–79.4)
Swelling of areae gastricae									
IC method	+	61	37	98	0.725	74.4	70.6	62.2	80.9
	–	21	89	110	(0.663–0.787)	(63.6–83.4)	(61.9–78.4)	(51.9–71.8)	(72.3–87.8)
Nodular change	+	6	2	8	0.52	5.3	98.8	75.0	59.4
	–	108	158	266	(0.498–0.542)	(2.0–11.1)	(95.6–99.8)	(34.9–96.8)	(53.2–65.4)
Patchy redness	+	32	30	62	0.547	28.1	81.4	51.6	61.5
	–	82	131	213	(0.496–0.598)	(20.1–37.3)	(74.5–87.1)	(38.6–64.5)	(54.6–68.1)
Red streak	+	1	25	26	0.574	0.9	84.4	3.8	54.7
	–	112	135	247	(0.544–0.603)	(0.0–4.8)	(77.8–89.6)	(0.1–19.6)	(48.2–61.0)
Erosion									
Flat	+	7	29	36	0.559	6.1	82.0	19.4	55.2
	–	107	132	239	(0.522–0.596)	(2.5–12.2)	(75.2–87.6)	(8.2–36.0)	(48.7–61.6)
Raised	+	7	29	36	0.599	6.2	82.0	19.4	55.5
	–	106	132	238	(0.522–0.596)	(2.5–12.3)	(75.2–87.6)	(8.2–36.0)	(48.9–61.9)
Hemorrhagic	+	1	4	5	0.508	0.9	97.5	20.0	58.1
	–	113	157	270	(0.493–0.523)	(6.0–4.8)	(93.8–99.3)	(0.5–71.6)	(52.0–64.1)
Bleeding spot	+	0	18	18	0.556	0.0	88.8	0.0	55.7
	–	113	160	273	(0.532–0.581)	(0.0–3.2)	(82.8–93.2)	(0.0–18.5)	(49.4–61.9)

+, present; –, absent. IC, indigocarmine; NPV, negative predictive value; PPV, positive predictive value; ROC/AUC, area under the curve of receiver operating characteristics.

for at least one of the three endoscopic findings: diffuse redness, spotty redness, and enlarged/tortuous folds, were judged as *H. pylori* positive, the sensitivity was 94.3%, specificity was 58.8%, and ROC/AUC was 0.815 (95% CI: 0.763–0.867). When the presence of two positive findings was judged as *H. pylori* positive, the sensitivity was 77.9% and the specificity was 72.6%, and when the presence of three positive findings was judged as *H. pylori* positive, sensitivity and specificity were 42.1% and 90.4%, respectively.

Nodular changes were noted in only two patients and the ROC/AUC was low (0.507, 95% CI: 0.497–0.517), being difficult to evaluate in this study. On the evaluation of swelling of the areae gastricae by the IC method, the ROC/AUC was 0.804 (95% CI: 0.747–0.861), higher than that on conventional endoscopy. Typical RAC[17] in the angle was noted in 69 patients and the ROC/AUC was 0.708 (95% CI: 0.659–0.756), not so high, but PPV was low (13.0%, 95% CI: 6.1–23.3). The ROC/AUC of fundic gland polyposis, hemorrhagic erosion, and bleeding spot was low (0.516–0.610), and PPV was low (8.8–16.7%).

Associations between the endoscopic findings in the antrum and *H. pylori* infection are shown in Table 4. Regarding the *H. pylori* infection-positive findings on conventional endoscopy, the ROC/AUC of mucosal swelling was 0.669 (95% CI: 0.610–0.727), followed by diffuse redness (0.646, 95% CI: 0.584–0.708). The frequency of spotty redness was lower (30.1%, 82/272), and the ROC/AUC was also low (0.525, 95% CI: 0.467–0.581). Nodular change was noted in only eight patients, similar to that in the corpus, and evaluation was difficult. The ROC/AUC of swelling of the areae gastricae by the IC method was 0.725 (95% CI: 0.663–0787, $P < 0.001$), being higher than those of all findings on conventional endoscopy. The ROC/AUC of red streak,[18] flat, raised, and hemorrhagic erosions, and bleeding spot was low (0.508–0.574), and PPV was low (0.0–20.0).

Regarding the association between the diagnosis of *H. pylori* infection of the entire stomach and each endoscopic finding, the parameters were similar to those of the association between the endoscopic findings in the corpus and *H. pylori* infection (Table 5).

Table 5 Diagnostic value of endoscopic features of the entire stomach for *H. pylori* infection

		H. pylori positive	*H. pylori* negative	Total	ROC/AUC (95% CI)	Sensitivity (%) (95% CI)	Specificity (%) (95% CI)	PPV (%) (95% CI)	NPV (%) (95% CI)
Diffuse redness	+	123	41	164	0.802	83.7	68.0	75.0	78.4
	–	24	87	111	(0.752–0.852)	(76.7–89.3)	(59.1–75.9)	(67.7–81.4)	(69.6–85.6)
Spotty redness	+	104	32	136	0.728	70.7	75.0	76.5	69.1
	–	43	96	139	(0.672–0.783)	(62.7–78.0)	(66.6–82.2)	(68.4–83.3)	(60.7–76.0)
Enlarged/tortuous fold	+	85	23	108	0.699	59.0	80.8	78.7	62.2
	–	59	97	156	(0.646–0.753)	(50.5–67.1)	(72.6–87.4)	(69.8–86.0)	(54.1–69.6)
Mucosal swelling	+	96	22	118	0.746	67.6	81.7	81.4	68.1
	–	46	98	144	(0.694–0.798)	(59.2–75.2)	(73.6–88.1)	(73.1–87.9)	(59.8–75.6)
Swelling of areae gastricae									
Conventional	+	80	19	99	0.735	64.0	83.0	80.8	67.4
	–	45	93	138	(0.680–0.790)	(54.9–72.4)	(74.8–89.5)	(71.7–88.0)	(58.9–75.1)
IC method	+	74	14	88	0.815	77.9	85.1	84.1	79.2
	–	21	80	101	(0.760–0.870)	(68.2–85.8)	(76.3–91.6)	(74.8–91.0)	(70.0–86.6)
Nodular change	+	2	0	2	0.507	1.4	100	100	47.2
	–	143	128	271	(0.497–0.516)	(2.0–4.9)	(97.2–100)	(15.8–100)	(41.2–53.4)
Patchy redness	+	44	17	61	0.585	30.3	86.7	72.1	52.4
	–	101	111	212	(0.538–0.633)	(23.0–38.5)	(79.6–92.1)	(59.2–82.9)	(45.4–59.2)
Red streak	+	8	28	36	0.582	5.4	78.1	22.2	41.8
	–	139	100	236	(0.542–0.623)	(2.4–10.4)	(70.0–84.9)	(10.1–39.2)	(35.5–48.4)
RAC	+	9	60	69	0.712	6.3	51.2	13.0	32.1
	–	133	63	196	(0.664–0.761)	(2.9–11.7)	(42.0–60.3)	(6.1–23.3)	(25.7–39.2)
Fundic gland polyposis	+	3	31	34	0.612	2.0	75.6	8.8.	40.0
	–	144	96	240	(0.573–0.651)	(0.4–5.8)	(67.2–82.8)	(1.9–23.7)	(33.8–46.5)
Erosion									
Flat	+	6	14	20	0.534	4.1	89.1	30.0	44.7
	–	141	114	255	(0.503–0.560)	(1.5–8.7)	(82.3–93.9)	(11.9–54.3)	(38.5–51.0)
Raised	+	5	5	10	0.503	3.4	96.1	50.0	46.4
	–	142	123	265	(0.480–0.525)	(1.1–7.8)	(91.1–98.7)	(18.7–81.3)	(40.3–52.6)
Hemorrhagic	+	1	5	6	0.516	0.7	96.1	16.7	45.7
	–	146	123	269	(0.498–0.534)	(0.0–3.7)	(91.1–98.7)	(0.4–64.1)	(39.7–51.9)
Bleeding spot	+	3	15	18	0.548	2.1	88.3	16.7	44.5
	–	141	113	254	(0.518–0.579)	(0.4–6.0)	(81.4–93.3)	(3.6–41.4)	(38.3–50.8)

+, present; –, absent. IC, indigocarmine; NPV, negative predictive value; PPV, positive predictive value; RAC, regular arrangement of collecting venules; ROC/AUC, area under the curve of receiver operating characteristics.

The diagnostic accuracy of a combination of two endoscopic findings was investigated. The numbers of patients analyzed were 180–208 and 255–274, using combinations including and not including the IC method, respectively, and *H. pylori* infection was diagnosed based on *H. pylori* infection of the entire stomach. On conventional endoscopy, a combination of diffuse redness in the corpus and mucosal swelling in the antrum was the most useful for diagnosing *H. pylori* infection, and the ROC/AUC rose to 0.812 (95% CI: 0.760–0.863). In cases concomitantly examined by the IC method, the ROC/AUC rose to 0.865 (95% CI: 0.813–0.917) when diffuse redness in the corpus on conventional endoscopy and swelling of the areae gastricae in the corpus by the IC method were combined, and 0.859 (95% CI: 0.808–09.10) when diffuse redness in the corpus on conventional endoscopy and swelling of the areae gastricae in the antrum by the IC method were combined.

DISCUSSION

IT IS SCIENTIFICALLY important to establish the endoscopic diagnosis of chronic gastritis with respect to the establishment of endoscopic findings corresponding to pathological findings internationally observed in accordance with

the Sydney System. In addition, this is also clinically important, because information such as progression of chronic gastritis and risk of gastric cancer development, important for future endoscopic follow up, is promptly provided.

Studies on the usefulness of magnifying endoscopy paying attention to micromucosal patterns and RAC for diagnosis of *H. pylori*-infected gastritis have recently been occasionally reported,[17,19,20] but findings on conventional endoscopy corresponding to pathological findings presented in the Sydney System have not yet been clarified, and the diagnosis of *H. pylori* infection by conventional endoscopy has not been established. Magnifying endoscopy is not necessarily appropriate for routine clinical practice because only a few facilities carry out magnifying endoscopy as a routine examination and a prolonged time is required, whereas conventional endoscopy is appropriate because it requires a shorter time. Endoscopists can evaluate the presence or absence of endoscopic findings, and *H. pylori* infection in gastric mucosa can be promptly diagnosed. Furthermore, expenses required for endoscopy only are able to be claimed; this procedure may be more cost-effective than the urease test with biopsy materials.

Endoscopic diagnosis of *H. pylori* infection in gastric mucosa by conventional endoscopy has not yet been established, and it is impossible to apply this procedure in clinical practice.[4–12] However, diagnostic performance for *H. pylori* infection with the new endoscopic findings introduced in the present study, such as diffuse redness, spotty redness, mucosal swelling, and swelling of the areae gastricae by the IC method, was favorable. The primary factor that improved the performance of diagnosing *H. pylori* infection in the present study may have been the appropriateness of the endoscopic findings as diagnostic indices. These new diagnostic indices could be clinically applied to endoscopic diagnosis of *H. pylori* infection.

In the present study, *H. pylori* infection was diagnosed by using microscopic observation of HE-stained preparations of biopsy specimens recommended by the Central Judgment Committee (Gifu, Japan) as a basic diagnostic tool, and immunostaining was additionally carried out in doubtful cases to make a final diagnosis. The diagnosis of *H. pylori* infection by microscopic observation of HE-stained preparations was doubtful and a definite diagnosis was made by additional immunostaining in three patients: two were *H. pylori* infection positive and one was negative.

Favorable consistency between the microscopic and serum antibody (anti-*H. pylori* IgG) methods showed that the microscopic method was considered valid as an *H. pylori* infection diagnosis tool.

Generally, redness, swelling, and pain are signs of tissue inflammation. The presence of redness and swelling in *H. pylori* infection-induced inflammation of the gastric mucosa has been endoscopically confirmed based on comparison with findings in *H. pylori*-eradicated cases.[21] Histologically, *H. pylori* infection induces hyperemia, edema, and cell infiltration in the gastric mucosa. Diffuse and spotty redness and enlarged and tortuous folds[22] in the corpus have been pointed out as typical conventional endoscopic findings corresponding to the histological findings. The ROC/AUC was 0.793 in diffuse redness, 0.725 in spotty redness, and 0.690 in enlarged/tortuous folds, showing that diffuse redness was a useful endoscopic finding in the *H. pylori*-infected stomach. Diffuse redness is readily diagnosed in the fundic gland mucosa because, compared to the pyloric gland mucosa, the mucosa is thick and rich in blood vessels,[23] in which inflammatory changes are easily observed. Histologically, diffuse redness is considered to reflect mucosal hyperemia, and a strong correlation with an objective index of redness, the hemoglobin index (IHb), has been reported, suggesting that diffuse redness is the most important feature for diagnosing *H. pylori* infection.[21] Spotty redness is considered to show a dilated collecting vein, but this finding alone is unlikely to serve as an index of *H. pylori* infection because its frequency was lower than that of diffuse redness and the ROC/AUC was also low. The ROC/AUC of enlarged/tortuous folds was low, but PPV was 76.9%, serving as a diagnostic index of *H. pylori* infection comparable to diffuse and spotty redness. In addition, when at least one of these three features (diffuse and spotty redness and enlarged/tortuous folds) was positive, *H. pylori* infection was positive at a sensitivity of 94.3%, suggesting the importance of paying attention to these three features for the evaluation. Additional evaluation of swelling of the areae gastricae in the corpus was also useful for diagnosing *H. pylori* infection.

In the antrum, the accuracy of diagnosing *H. pylori* infection was lower than that in the corpus, showing the limitation of the dependence on conventional endoscopic findings alone. *H. pylori* infection induces chronic gastritis in the antrum and it advances to the corpus. Histological changes also first appear in the antrum, such as mucosal atrophy and intestinal metaplasia, and marked mucosal unevenness is also observed in this region on endoscopy. Accordingly, diffuse redness and swelling of the areae gastricae, which are important for diagnosing *H. pylori* infection in the corpus, are not necessarily readily diagnosed in the antrum on conventional endoscopy, and these are unlikely to be useful diagnostic indices of *H. pylori* infection.

The IC method that we introduced in the present study is a superior endoscopic method of clarifying mucosal unevenness. This method clarifies the morphology of the areae gastricae and readily diagnoses swelling of the areae gastricae. Particularly, the diagnostic accuracy of the swelling of

the areae gastricae was highest in the antrum, in which diagnostic performance for *H. pylori* infection was poor. This shows that the IC method may be very useful and, in the future, it should be conducted in all patients.

Nodular change has been reported as a useful feature of *H. pylori* infection in gastric mucosa.[24] However, it was difficult to evaluate in this study because of less frequent observation.

For the actual diagnosis of *H. pylori* infection, it is necessary to first evaluate the presence or absence of diffuse redness in the corpus. When this evaluation is difficult, attention should be paid to spotty redness, enlarged/tortuous folds, and swelling of the areae gastricae. Facilities capable of carrying out the IC method should investigate swelling of the areae gastricae. When these findings are observed as a complex, the diagnostic accuracy further increases. When the diagnosis of *H. pylori* infection in the corpus is difficult, or when *H. pylori* infection is judged as negative, it is necessary to evaluate other features in the antrum, particularly paying attention to the presence or absence of swelling of the areae gastricae by the IC method.

In contrast, RAC, red streak, fundic gland polyposis, hemorrhagic erosion, and bleeding spot in the corpus and red streak, hemorrhagic erosion, bleeding spot, and raised and flat erosions[8,9] in the antrum have been pointed out as findings suggesting negative *H. pylori* infection. In our study, RAC was useful as a relatively frequent *H. pylori* infection-negative finding (PPV: 13.0%) in the corpus. RAC is clearly observed on magnifying endoscopy, but it can also be diagnosed by observation at a close site using a high-resolution conventional endoscope.[3] In addition, the endoscopic findings of fundic gland polyposis, hemorrhagic erosion and bleeding spot in the corpus and red streak, flat and raised erosions, hemorrhagic erosion and bleeding spot in the antrum can be used as suggesting negative *H. pylori* infection in endoscopic diagnosis.

The present study had limitations. Prior to this study, each endoscopic finding was explained in order to standardize endoscopic findings and unify the accuracy of diagnosis among hospitals/physicians participating in this study, whereas the assessment of endoscopic findings depended on each endoscopist.

In conclusion, the present study suggested that endoscopic diagnosis of *H. pylori* infection in gastric mucosa by conventional and IC methods is mostly possible.

ACKNOWLEDGMENT

THE STUDY WAS supported by a grant from the Japanese Foundation for Research and Promotion of Endoscopy.

CONFLICT OF INTERESTS

AUTHORS DECLARE NO conflict of interests for this article.

REFERENCES

1 Price AB. The Sydney system; Histological division. *J. Gastroenterol. Hepatol.* 1991; **6**: 209–22.
2 Dixson MF, Genta RM, Yardley JH, Correa P. Classification and grading of gastritis. The updated Sydney System. International workshop on the histopathology of gastritis, Houston 1994. *Am. J. Surg. Pathol.* 1996; **20**: 1161–81.
3 Yan SL, Wu ST, Chen CH *et al.* Mucosal patterns of *Helicobacter pylori*-related gastritis without atrophy in the gastric corpus using standard endoscopy. *World J. Gastroenterol.* 2010; **16**: 496–500.
4 Rede'en S, Petersson F, Jo'nsson KA, Borch K. Relationship of gastroscopic features to histological findings in gastritis and *Helicobacter pylori* infection in a general population sample. *Endoscopy* 2003; **35**: 946–50.
5 Bah A, Saraga E, Armstrong D *et al.* Endoscopic features of *Helicobacter pylori*-related gastritis. *Endoscopy* 1995; **27**: 593–6.
6 Calabrese C, Di Febo G, Brandi G *et al.* Correlation between endoscopic features of gastric antrum, histology and *Helicobacter pylori* infection in adults. *Ital. J. Gastroenterol. Hepatol.* 1999; **31**: 359–65.
7 Lehmann FS, Renner EL, Meyer-Wyss B *et al. Helicobacter pylori* and gastric erosions. Results of a prevalence study in asymptomatic volunteers. *Digestion* 2000; **62**: 82–6.
8 Elta GH, Appelman HD, Behler EM, Wilson JA, Nosrant TJ. A study of the correlation between endoscopic and histological diagnosis in gastroduodenitis. *Am. J. Gastroenterol.* 1987; **82**: 749–53.
9 Hilker E, Domeschke W, Stoll R. ^{13}C-urea breath test for detection of *Helicobacter pylori* and its correlation with endoscopic and histologic findings. *J. Physiol. Pharmacol.* 1996; **47**: 79–90.
10 Laine L, Cohen H, Sloane R, Marin-Sorensen M, Weinstein WM. Interobserver agreement and predictive value of endoscopic findings for *H. pylori* and gastritis in normal volunteers. *Gastrointest. Endosc.* 1995; **42**: 420–3.
11 Yela MC, Manzano ML, Rodrigues-Munoz S *et al.* Assessment of the usefulness of endoscopic signs in *Helicobacter pylori* associated gastritis. *Rev. Esp. Enferm. Dig.* 1997; **89**: 3–12.
12 Khakoo SI, Lobo AJ, Shepherd NA, Wilkinson SP. Histological assessment of the Sydney classification of endoscopic gastritis. *Gut* 1994; **35**: 1172–5.
13 Ida K, Tada M. *Chromoscopy. Special Method and Techniques in Gastroenterologic Endoscopy*. Philadelphia, PA: WB Saunders, 1987; 203–20.
14 Ida K, Kohli Y, Shimamoto K, Hashimoto Y, Kawai K. Endoscopic findings of fundic and pyloric gland area using dye scattering method. *Endoscopy* 1973; **5**: 21–6.

15 Kikuchi S, Miwa H. Efficacy of direct ELISA kit E Plate 'Eiken' *H. pylori* antibody on diagnosis of *Helicobacter pylori* infection. *Jpn. J. Med. Pharm. Sci.* 2000; **43**: 581–6. (in Japanese.)
16 Watanabe H, Hayama T, Ohya T *et al.* Comparison of *Helicobacter pylori* detection rate between hematoxylin-eosin stained sections and Giemsa stained sections. *Jpn. J. Helicobacter Res.* 2007; **9**: 77–9. (in Japanese.)
17 Yagi K, Nakamura A, Sekine A. Characteristic endoscopic and magnified endoscopic findings in the normal stomach without *Helicobacter pylori* infection. *J. Gastroenterol. Hepatol.* 2002; **17**: 39–45.
18 Kawabe T, Maeda S, Ogura K *et al.* Antral red streaking is a negative endoscopic sign for *Helicobacter pylori* infection. *Dig. Endosc.* 2002; **14**: 87–92.
19 Yagi K, Nakamura A, Sekine A. Comparison between magnifying endoscopy and histological, culture and urease test findings from the gastric mucosa of the corpus. *Endoscopy* 2002; **34**: 376–81.
20 Gonen C, Simsek I, Sarioglu S, Akpinar H. Comparison of high resolution magnifying endoscopy and standard videoendoscopy for the diagnosis of *Helicobacter pylori* gastritis in routine clinical practice: A prospective study. *Helicobacter* 2009; **14**: 12–21.
21 Uchiyama K, Ida K, Okuda J *et al.* Correlation of Hemoglobin Index (IHb) of gastric mucosa with *Helicobacter pylori (H. pylori)* infection and inflammation of gastric mucosa. *Scand. J. Gastroenterol.* 2004; **11**: 1054–60.
22 Mihara M, Haruma K, Kamada T *et al.* The role of endoscopic findings for the diagnosis of *Helicobacter pylori* infection: Evaluation in a country with high prevalence of atrophic gastritis. *Helicobacter* 1999; **1**: 40–8.
23 Hattori T. On cell proliferation and differentiation of fundic mucosa of the golden Hamster. *Cell Tissue Res.* 1974; **148**: 213–26.
24 Loffeld RJ. Diagnostic value of endoscopic signs of gastritis with special emphasis to nodular gastritis. *Neth. J. Med.* 1999; **54**: 96–100.

Digestive Endoscopy 2013; ••: ••–•• doi: 10.1111/den.12032

Original Article

Endoscopic diagnosis of gastric intestinal metaplasia: A prospective multicenter study

Nobuhiro Fukuta,[1] Kazunori Ida,[1] Takahiro Kato,[1] Noriya Uedo,[2] Takashi Ando,[3] Hidenobu Watanabe,[4] Takuro Shimbo[5] and *Study Group for Investigating Endoscopic Diagnosis of Gastric Intestinal Metaplasia

[1]*Department of Gastroenterology, Murakami Memorial Hospital, Asahi University, Gifu,* [2]*Department of Gastroenterology, Osaka Medical Center for Cancer and Cardiovascular Diseases, Osaka,* [3]*Department of Gastroenterology, Social Insurance Kyoto Hospital, Kyoto,* [4]*Department of Pathology, Niigata University, Niigata and* [5]*Department of Clinical Research and Informatics, International Clinical Research Center, Research Institute, Institute Medical Center of Japan, Tokyo, Japan*

Background: Intestinal metaplasia (IM) of the gastric mucosa has long attracted attention as a premalignant lesion involved in gastric carcinogenesis. However, endoscopic diagnosis of IM has remained unclear for a long time. In recent years, the methylene blue staining technique and narrow-band imaging (NBI) magnifying endoscopy have facilitated clinical diagnosis of IM, although these methods have some problems due to their complexity. Simple methods for diagnosis of IM using conventional endoscopy and the indigo carmine contrast (IC) method are necessary.

Patients and Methods: This study was a multicenter, prospective, randomized, comparative study involving 10 facilities. The appearance of IM was examined using conventional and IC methods with an electronic endoscope.

Results: Subjects included 163 patients, of whom 87 and 76 underwent conventional and IC methods, respectively. Sensitivity, specificity, and receiver operating characteristic/area under the curve (ROC/AUC) of conventional and IC methods for the detection of IM in the gastric antrum showed that diagnostic performance of the conventional method was higher, but not significantly, than that of the IC method. Sensitivity, specificity and ROC/AUC of conventional and IC methods for the detection of IM in the gastric body showed that the IC method yielded better (but not significantly better) results than the conventional method.

Conclusion: The diagnostic performance of the conventional method did not significantly differ from that of the IC method. A villous appearance, whitish mucosa, and rough mucosal surface, as observed by both methods, and areae gastricae pattern, as observed by the IC method, were useful indicators for endoscopic diagnosis of IM.

Key words: contrast method, conventional method, endoscopic diagnosis, intestinal metaplasia

INTRODUCTION

INTESTINAL METAPLASIA (IM) of the gastric mucosa has attracted attention as a premalignant or possible premalignant lesion involved in gastric carcinogenesis since the early 1900s.[1] In recent years, *Helicobacter pylori* (*H. pylori*) has been classified as a definite carcinogen in gastric cancer.[2] In a follow-up study of patients, Uemura *et al.*[3] demonstrated that *H. pylori*-positive patients, but not their negative counterparts, developed gastric cancer. However, it has been reported that *H. pylori* eradication suppresses the development of metachronous gastric cancer, but that gastric cancer occurs more frequently in those with extensive atrophy of the stomach.[4,5] These findings suggest that gastric cancer arises from IM with marked gastric atrophy even after *H. pylori* eradication. Mutoh *et al.* demonstrated that gastric cancer arose from experimentally induced IM

Corresponding: Nobuhiro Fukuta, Department of Gastroenterology, Murakami Memorial Hospital, Asahi University, 3-23, Hashimoto-cho, Gifu 500-8523, Japan. Email: nobu-fukuta@mbh.nifty.com

*Study Group for Investigating Endoscopic Diagnosis of Gastric Intestinal Metaplasia: *President*: Kazunori Ida (Gifu); *Managers*: Mototsugu Kato (Sapporo), Takahiro Kato (Gifu), Sachiyo Nomura (Tokyo), Shuichi Ohara (Sendai), Nobuhiro Sakaki (Tokyo), Takuro Shimbo (Tokyo), Noriya Uedo (Osaka), Naomi Uemura (Tokyo), Hidenobu Watanabe (Niigata); *Advisors*: Michio Kaminishi (Tokyo), Kazumasa Miki (Tokyo), Saburou Nakazawa (Nagoya), Hirohumi Niwa (Tokyo), Masaharu Tatuta (Osaka); *Contributors*: Takashi Ando (Kyoto), Masanori Ito (Hiroshima), Kazunari Murakami (Oita), Masaaki Kodama (Oita), Shigemi Nakajima (Ootsu), Hiroyoshi Ota (Matsumoto), Shuichi Terao (Kakogawa), Nobuaki Yagi (Kyoto), Norimasa Yoshida (Kyoto).

Received 19 August 2012; accepted 29 November 2012.

without *H. pylori* infection. Many studies have been conducted based on these findings.[6–13]

However, IM had escaped endoscopic diagnosis for a long period of time until 1966, when Takemoto first demonstrated by gastro-fiberscopy that the presence of grayish-white elevations scattered on the mucosa of the pyloric antrum and gastric angle was a finding of IM, and termed it special-type IM.[14] In 1968, Yokoyama reported the same type of IM at the 3rd Asian Pacific Congress of Gastroenterology.[15] However, the frequency of this type of lesion was so low that it was not an endoscopic finding typical of IM.

In contrast, the methylene blue staining method originated by Ida *et al.*,[16] a type of chromoendoscopy developed in 1975, facilitated diagnosis of IM.[17,18] Although this was revolutionary as a method for endoscopic diagnosis of IM, accurate diagnosis of IM requires the adequate removal of mucus, making its general use in clinical practice cumbersome, thus hampering its widespread use. In 2006, Uedo *et al.*[19] reported that narrow-band imaging (NBI) with magnifying endoscopy yielded excellent diagnostic results.

Advances in these specialized techniques and new imaging modalities enabled endoscopic diagnosis of IM. However, we consider that simple methods for diagnosis of IM using conventional endoscopy are preferable in daily clinical practice and attempted to diagnose IM using high-resolution electronic endoscopes exhibiting higher performance than conventional ones. In addition, for comparison, we also carried out diagnosis of IM using the indigocarmine contrast (IC) method,[20] which enables visualization of the minute irregularities of the mucosal surface and the areae gastricae pattern without using special endoscopic equipment. In addition, the IC method using conventional endoscopy followed by simple IC solution spray is suitable for routine clinical diagnosis of IM.

METHODS

Patients

THE PRESENT STUDY was a multicenter, prospective, randomized, comparative study involving 10 facilities. Expert endoscopists with more than 15 years of experience participated in this study. Subjects were patients who were registered with the Secretariat, located in Asahi University Murakami Memorial Hospital, between January 2009 and January 2010. In view of the results of a pilot study, the target number of patients to be enrolled was 100 each for conventional and IC method groups. Patients were randomly assigned to one of the two groups according to a random number table provided for each center to facilitate intergroup comparisons, after adjusting for patient characteristics, including unknown confounding factors influencing the interpretation of endoscopic findings.

Criteria for subject selection were as follows: (i) patients at least 40 years old for whom the attending physician needed to carry out endoscopy in routine practice; and (ii) patients giving written informed consent to participate in this study. Exclusion criteria were: (i) patients with advanced (or suspected advanced) cancer; (ii) patients with suspected acute gastric bleeding or perforation; (iii) patients previously diagnosed with or without IM; (iv) gastrectomized patients; (v) patients who took NSAIDs, anticoagulants, or antiplatelet agents within 7 days of endoscopy; (vi) patients with dysfunction of vital organs; and (vii) pregnant patients.

Upon enrollment, patients at each facility were assigned an identification number and date of report, name of facility, date of examination, gender, age, disease name, and endoscopic diagnosis. These were reported to the secretariat of the study group by fax within 3 days of the date of examination before histopathological findings became evident.

This study was carried out after approval by the Ethics Committee of each facility.

Endoscopic examination

Only Olympus (Tokyo, Japan) endoscopes (high-resolution EVIS-240 or any of the EVIS-260 series) were used to minimize inter-facility differences in image quality, including color tone.

At the start of this study, characteristic findings of IM were obtained from many patients in whom the presence of IM had been confirmed. The endoscopic findings were classified into six types, and as all of them are frequently observed by endoscopy and are not unusual or specific findings, endoscopy-based diagnosis was readily established, and each endoscopist in the study group tried to gain a full understanding of each endoscopic finding. The study was started after a pilot study on the endoscopic diagnosis of IM in 10 patients was carried out at each center, showing that the conventional and IC methods exhibited a favorable diagnostic performance. To share understanding about each endoscopic finding, books of photographs were made, which were distributed to the participating centers.

Biopsies were taken at the antral lesser curvature (2–3 cm proximal to the pyloric ring) and gastric corpus lesser curvature (approximately 4 cm proximal to the gastric angle). In the IC-method group, an indigocarmine solution was sprayed under direct vision mainly on the site to be evaluated, and the contrast image was observed. In both diagnostic methods, evaluation sites were examined for the features of

IM described below at the closest distance of biopsy point. This study was concerned with the diagnosis of endoscopically visible IM; that is, IM lesions of a certain size, and did not aim to diagnose focal microscopic IM.

In the conventional method, the following endoscopic findings were used as indicators for the diagnosis of IM: whitish mucosa (Fig. 1), a rough mucosal surface or uneven mucosal surface (Fig. 2), a villous appearance (Fig. 3), atypical collecting venules (CV) showing an abnormal morphology and uneven distribution (Fig. 4), and patchy redness (Fig. 5).

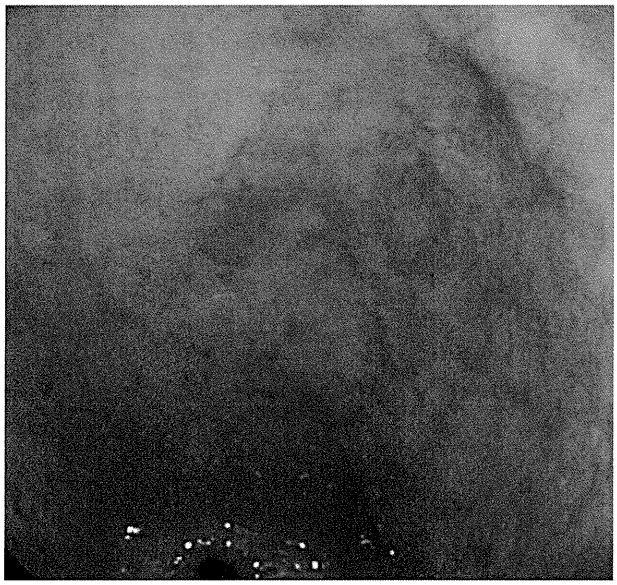

Figure 1 Whitish mucosa is irregularly clustered (antrum).

In the IC method, areae gastricae patterns in the pyloric gland region and intermediate zone (and the above-described findings) were used as indicators for diagnosis of IM. Classification of areae gastricae patterns, P_0, P_1, P_2, and P_3, as described by Ida and Tada[21] was used in this study. Areae gastricae patterns have been reported to be correlated with atrophic changes in the gastric mucosa. As shown in Figure 6, patterns have been classified to four types. The width of grooves between areae gastricae becomes wider as the type of areae gastricae changes from type 0 to type 3, and areae gastricae are classified according to the degree of irregularity in the groove width and size and shape of areae gastricae. Figure 7 shows the endoscopic appearance of areae gastricae. In types P_2 and P_3, areae gastricae showed atrophic changes, often with a villous appearance on their surface or grooves between areas (Fig. 8). In the mucosa of the intermediate zone of the gastric corpus lesser curvature, the presence of type P_2/P_3-like areae gastricae and a diffuse, villous mucosal pattern was considered a diagnostic indicator of IM (Fig. 8).

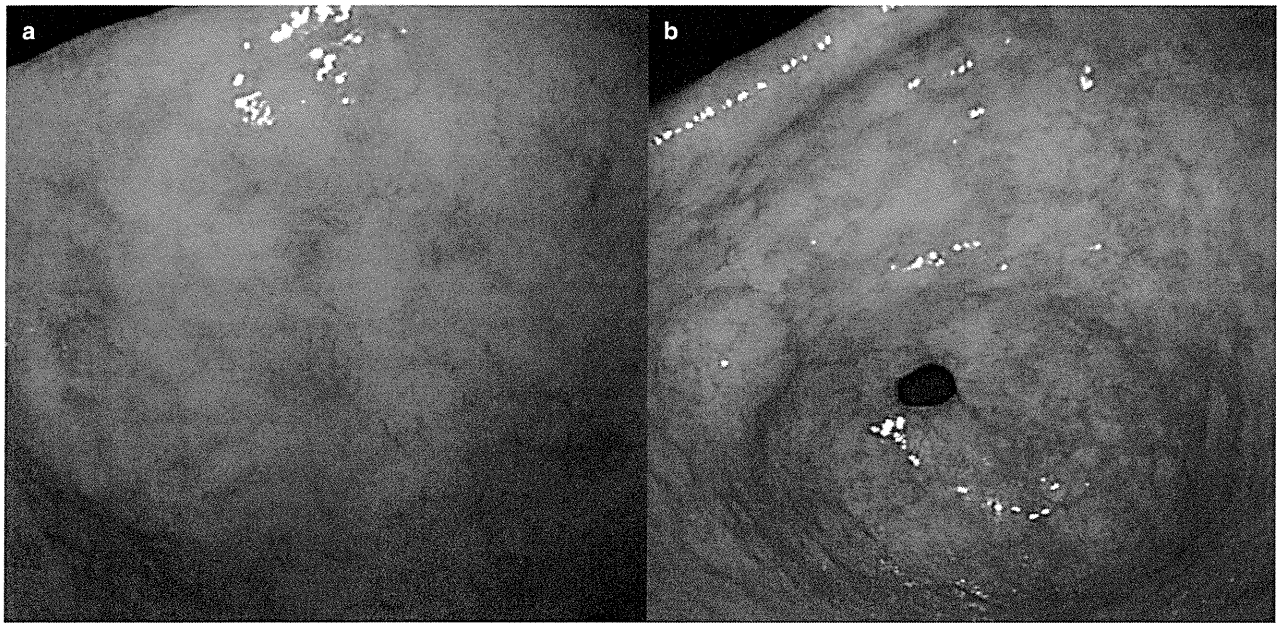

Figure 2 (a) Rough-surfaced mucosa (antrum). (b) Uneven-surfaced mucosa (antrum). Whitish, granules of different sizes and shapes are seen scattered.

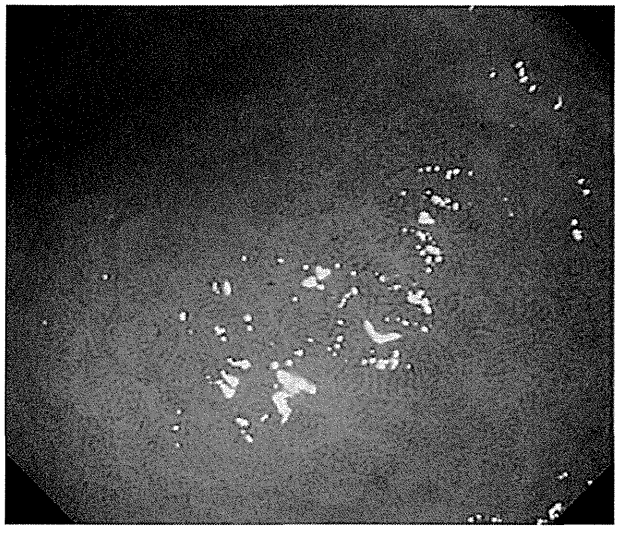

Figure 3 Villous appearance (antrum).

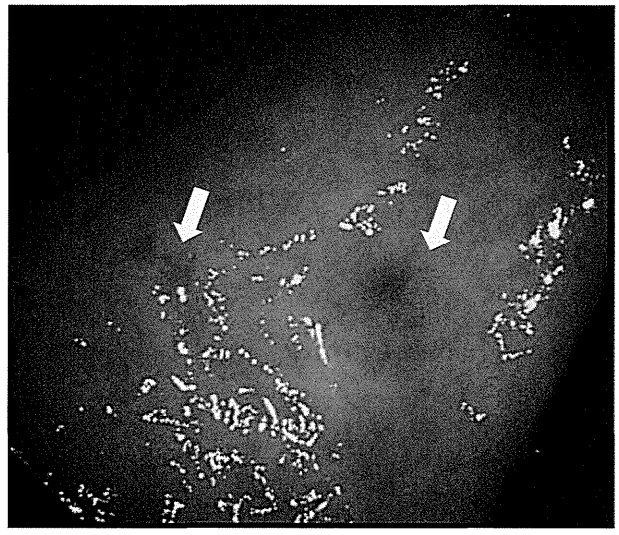

Figure 5 Patchy redness (angle; arrows).

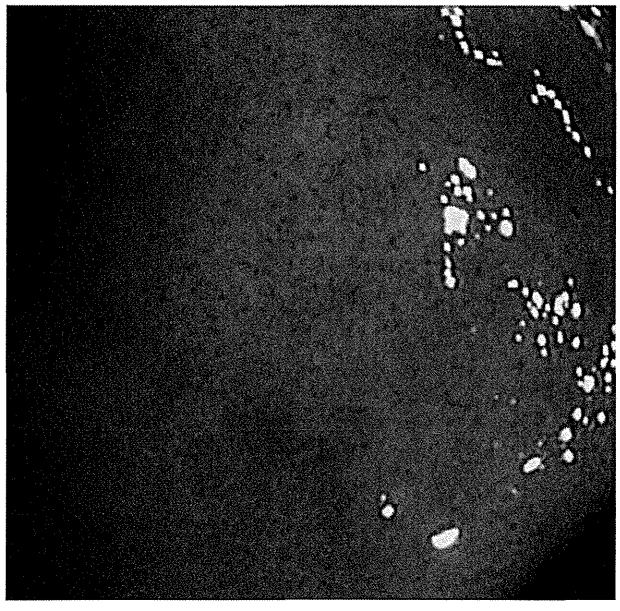

Figure 4 Atypical collecting venule showing an irregular shape and uneven distribution.

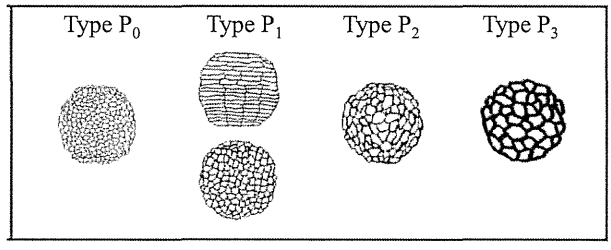

Figure 6 Schema of areae gastricae type by the indigocarmine method. Type P_0: areae gastricae are fine, densely arranged, and divided by very narrow grooves. Type P_1: areae gastricae are Tatami mat-shaped, arranged in a grid pattern, or nearly circular in shape. Grooves are narrow and densely arranged. Types P_2 and P_3: areae gastricae are irregular in shape and size. In type P_3, these findings are more marked, and areae gastricae are irregular in shape and size and separated by grooves of irregular width, and have a villous appearance.

Histological examination

Immediately after endoscopic diagnosis of IM, a biopsy specimen was taken from each of the sites for evaluation (the lesser curvature of the gastric antrum and body) and diagnosed for the presence or absence of IM according to the updated Sydney System.[22]

Hematoxylin-eosin (HE)-stained sections of biopsies were prepared and used for histopathological diagnosis at each facility. At a later date, histological specimens were given an anonymous identification number and sent to a blinded pathologist with more than 40 years of experience, who made all pathological diagnoses and sent the results to the secretariat.

Statistical analysis

Using the presence or absence of IM in biopsies as the gold standard, results of endoscopic diagnosis were compared by site and method. In parallel, a combination of the final diagnosis by the attending physician and more than one endoscopic finding was considered. The diagnostic performance

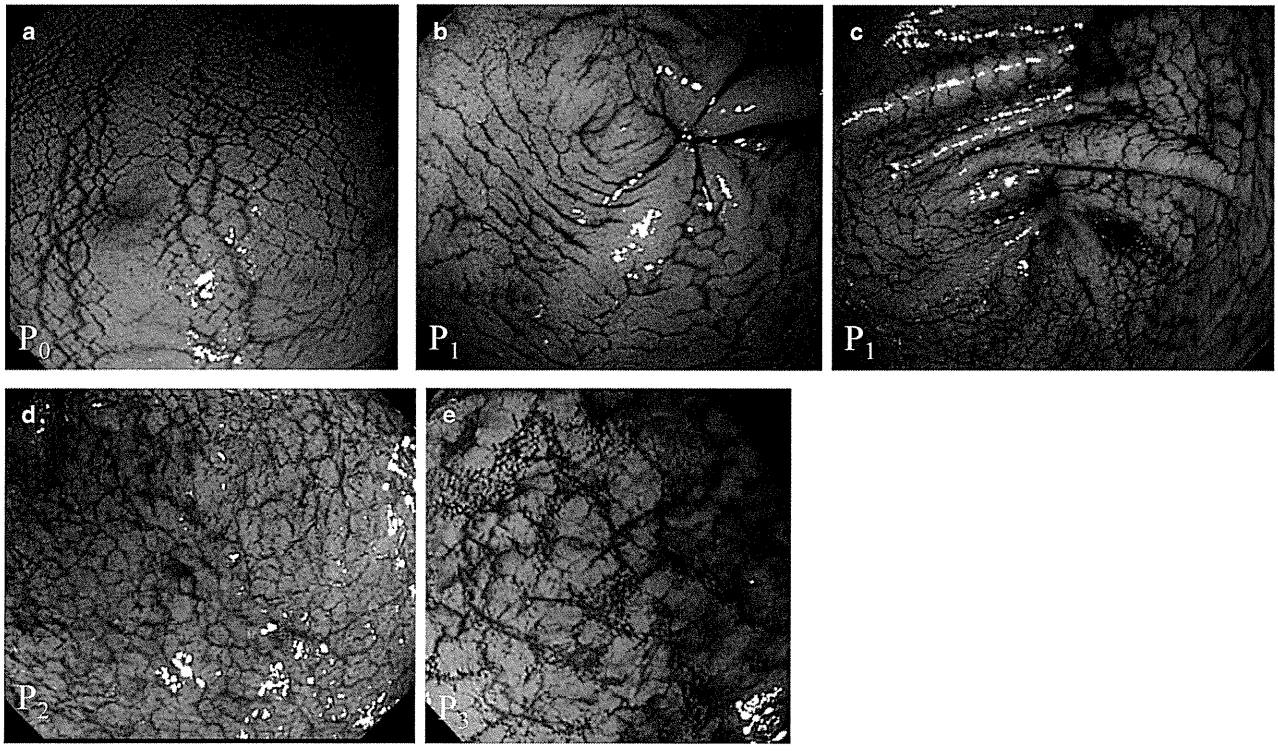

Figure 7 Endoscopic figures of areae gastricae (indigocarmine method).

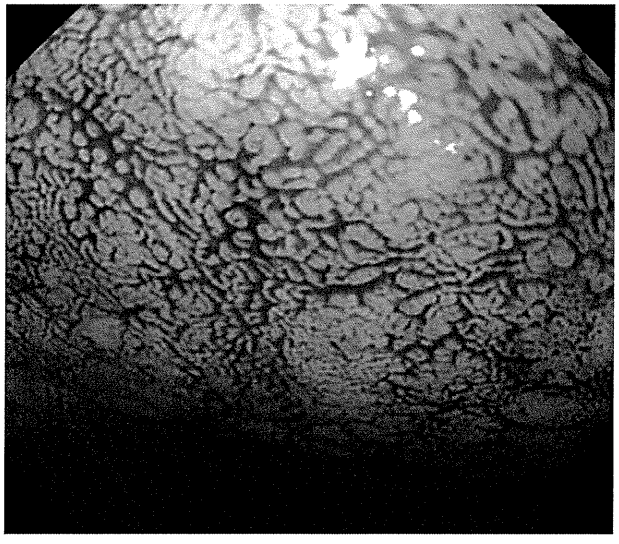

Figure 8 Typical villous appearance (body) (indigocarmine method).

of endoscopy was evaluated in terms of sensitivity, specificity, receiver operating characteristic/area under the curve (ROC/AUC) value, positive-predictive value (PPV), and negative-predictive value (NPV). When more than one endoscopic finding was combined, the ROC-AUC was calculated based on logistic regression analysis.

RESULTS

AS ONE OF the 164 registered patients was ineligible, 163 were included in the study. At the baseline, 90 patients (55.2%) were male, and 73 (44.8%) were female, with a mean age of 66 years (range, 41–85 years). Eighty-seven (53.4%) and 76 (46.6%) patients were assigned to conventional and IC methods, respectively. No significant differences were found in baseline data between the two groups.

Seventy-six patients (46.6%) had chronic gastritis, 29 (17.8%) had gastric or duodenal ulcer (including scars), 26 (16.0%) had early gastric cancer, 27 (16.6%) had other diseases, and five (3.1%) had no description of their disease.

Table 1 shows the results of endoscopic diagnosis of IM in the gastric antrum by conventional and IC methods corresponding to pathological diagnosis. The sensitivity, specificity, and ROC/AUC of conventional and IC methods were 94.6%, 69.1%, and 0.818; and 78.4%, 57.9%, and 0.682, respectively, showing no significant differences in diagnostic performance between the two methods for diagnosis of IM in the gastric antrum.

Table 1 Diagnostic results of intestinal metaplasia in the gastric antrum

	%	95% CI (exact method) %	
Conventional method			
Sensitivity	94.6	81.8	99.3
Specificity	69.1	52.9	82.4
PPV	72.9	58.2	84.7
NPV	93.6	78.6	99.2

	%	95% CI (exact method) %	
IC method			
Sensitivity	78.4	64.7	88.7
Specificity	57.9	33.5	79.8
PPV	83.3	69.8	92.5
NPV	50.0	28.2	71.8

	n	ROC/AUC	SE	95% CI		*P*-value
Conventional method	79	0.818	0.041	0.738	0.898	0.075
IC method	70	0.682	0.065	0.554	0.809	

CI, confidence interval; IC, indigocarmine; NPV, negative predictive value; PPV, positive predictive value; ROC/AUC, receiver operating characteristic/area under the curve.

Table 2 Diagnostic results of intestinal metaplasia in the gastric body

	%	95% CI (exact method) %	
Conventional method			
Sensitivity	86.1	70.5	95.3
Specificity	65.9	50.1	79.5
PPV	67.4	52.0	80.5
NPV	85.3	68.9	95.1

	%	95% CI (exact method) %	
IC method			
Sensitivity	86.0	73.3	94.2
Specificity	82.6	61.2	95.1
PPV	91.5	79.6	97.6
NPV	73.1	52.2	88.43

	n	ROC/AUC	SE	95% CI		*P*-value
Conventional method	80	0.760	0.047	0.669	0.851	0.212
IC method	73	0.843	0.047	0.750	0.936	

CI, confidence interval; IC, indigocarmine; NPV, negative predictive value; PPV, positive predictive value; ROC/AUC, receiver operating characteristic/area under the curve.

Table 3 Endoscopic findings of intestinal metaplasia

Antrum	Conventional method				IC method			
	n	ROC/AUC	95% CI		*n*	ROC/AUC	95% CI	
Whitish mucosa	82	0.752	0.666	0.838	75	0.676	0.555	0.797
Rough mucosal surface	82	0.752	0.666	0.838	75	0.688	0.568	0.807
Atypical collecting venule	81	0.700	0.612	0.787	74	0.616	0.517	0.715
Villous appearance	69	0.800	0.702	0.897	73	0.770	0.665	0.876
Patchy redness	82	0.598	0.491	0.706	74	0.532	0.403	0.660
Areae gastricae pattern					74	0.746	0.623	0.868
Body	Conventional method				IC method			
	n	ROC/AUC	95% CI		*n*	ROC/AUC	95% CI	
Whitish mucosa	81	0.741	0.652	0.831	73	0.772	0.662	0.883
Rough mucosal surface	80	0.758	0.667	0.849				
Atypical collecting venule	81	0.701	0.603	0.798				
Villous appearance	73	0.703	0.598	0.808	74	0.774	0.669	0.878
Patchy redness	82	0.552	0.444	0.660	74	0.581	0.460	0.702
Areae gastricae pattern					73	0.895	0.805	0.986

CI, confidence interval; IC, indigocarmine; ROC/AUC, receiver operating characteristic/area under the curve.

Table 2 shows the results of endoscopic diagnosis of IM in the gastric body by conventional and IC methods. The sensitivity, specificity, and ROC/AUC of conventional and IC methods were 86.1%, 65.9%, and 0.760; and 86.0%, 82.6%, and 0.843, respectively, showing no significant differences in diagnostic performance between the two methods for diagnosis of IM in the gastric body.

Table 3 shows the results of endoscopic diagnosis of IM in the gastric antrum and body based on endoscopic findings (as indicators of IM) by conventional and IC methods, as

assessed by ROC/AUC. ROC/AUC of the conventional method for detection of a villous appearance in the gastric antrum was the highest, at 0.800, followed by 0.752 for the detection of a whitish mucosa and rough mucosal surface. ROC/AUC for the detection of atypical CV and patchy redness was low, at 0.699 and 0.598, respectively. ROC/AUC of the IC method for detection of a villous pattern was also the highest, at 0.770, followed by 0.746 for the areae gastricae pattern, 0.688 for a rough mucosal surface, 0.676 for a whitish mucosa, 0.616 for CV-like structures, and 0.532 for patchy redness.

ROC/AUC of the conventional method for detection of a villous pattern in the gastric body was somewhat lower, at 0.703, than that in the gastric antrum, but ROC/AUC values for other endoscopic findings were almost the same as those for the gastric antrum. In contrast, ROC/AUC of the IC method for the areae gastricae pattern was the highest, at 0.895, followed by 0.774 for a villous pattern and 0.772 for a whitish mucosa. The diagnostic performance of the IC method for the detection of indicators of IM, such as CV-like structures and patchy redness, in the gastric body was also low. A combination of a villous pattern and whitish mucosa or the associated rough mucosal surface, which are important diagnostic indicators in the conventional method, increased the ROC/AUC to 0.852. A combination of a villous pattern and areae gastricae pattern in the gastric body increased the ROC/AUC to 0.919.

When types P_0 and P_1 areae gastricae patterns (with slight atrophic changes) and types P_2 and P_3 areae gastricae patterns (with marked atrophic changes), as determined by the IC method, were compared regarding sensitivity, specificity, and other parameters (Table 4), the sensitivity, specificity, PPV, and NPV of the IC method were very high, at 0.8, 0.6, 0.8, and 0.5 in the gastric antrum, and 0.9, 0.8, 0.9, and 0.9 in the gastric body, respectively. A combination of a villous pattern and whitish mucosa or the associated rough mucosal surface in the gastric antrum (as important diagnostic indicators in the conventional method) increased the ROC/AUC to 0.852, and a combination of a villous pattern and areae gastricae pattern in the gastric body, as detected by the IC method, increased the ROC/AUC to 0.919.

Table 4 Comparison between types P_0 and P_1 areae gastricae and types P_2 and P_3 areae gastricae

Areae gastricae pattern	IM negative	IM positive	Total	Sensitivity	95% CI_low	Specificity	95% CI_low	PPV	95% CI_low	NPV	95% CI_low
Antrum											
P_0, P_1	11	10	21	0.80	0.669	0.550	0.315	0.820	0.686	0.524	0.298
P_2, P_3	9	41	50					0.769	0.914		0.743
Total	0	51	71								
Body											
Areae gastricae pattern	IM negative	IM positive	Total	Sensitivity	95% CI_low	Specificity	95% CI_low	PPV	95% CI_low	NPV	95% CI_low
P_0, P_1	16	2	18	0.95	0.838	0.760	0.528	0.889	0.759	0.889	0.653
P_2, P_3	5	40	45					0.918	0.963		0.986
Total	21	42	63								

CI, confidence interval; IM, intestinal metaplasia; NPV, negative predictive value; PPV, positive predictive value.

DISCUSSION

IN 1966, TAKEMOTO *et al.* first described in Japanese the presence of grayish-white elevations scattered on the mucosa of the pyloric antrum and gastric angle as a finding of a specific type of IM. In 1968, Yokoyama[15] reported these findings. However, the observed frequency of this type of IM was low, and could not generally be used in clinical diagno-

sis. Kaminishi *et al.*[23] reported that the sensitivity of conventional endoscopy for the detection of IM lesions was low, at 6%.

The methylene blue staining method,[16] a type of chromoendoscopy developed in 1975, facilitated endoscopic diagnosis of IM, resulting in the reporting of excellent results with Kawai *et al.*[24] reporting a sensitivity of 91.2% and a specificity of 87.5%. Although this was an epoch-making method for the endoscopic diagnosis of IM, its accurate diagnosis requires pretreatments, such as mucus removal, thus hampering its widespread use. Recently, Uedo *et al.*[19] reported that NBI with magnifying endoscopy yielded favorable results in the diagnosis of IM based on the finding of a light blue crest, with a sensitivity of 89% and a specificity of 93%.

However, IM is classified as a lesion of paramount clinical importance involved in gastric carcinogenesis, and it is desirable for IM to be easily diagnosable in daily clinical practice. Thus, we compared conventional and IC methods for IM diagnosis using a recently developed high-resolution electronic endoscope. The present study reports the first multicenter prospective study in the world on endoscopic diagnosis of IM. We consider that the various findings presented in this paper facilitate the general endoscopic diagnosis of IM.

The diagnostic performance of the conventional method, as assessed by ROC/AUC, for the detection of IM in the gastric antrum was higher than that of the IC method, and that of the IC method for the detection of IM in the gastric body was higher than the conventional method. Similar results were obtained in terms of sensitivity and specificity: the sensitivity and NPV of the conventional method for the detection of IM in the gastric antrum were very high, at 94.6 and 93.6%, respectively. In the gastric body, the sensitivity and specificity of the IC method were higher, and the PPV was high, at 91.5%.

The ROC/AUC values of a whitish mucosa and rough mucosal surface in the gastric antrum, observed using IC, were low, but those of a villous appearance and areae gastricae pattern were 0.770 and 0.746, respectively, showing a significant diagnostic performance. The diagnostic rate of a whitish mucosa in the gastric body was relatively high, and the blue color of indigocarmine solution did not interfere with observation of the mucosal color. In addition, the ROC/AUC of the areae gastricae pattern visualized by the IC method was the highest, at 0.895, indicating that the areae gastricae pattern is an extremely useful diagnostic indicator.

Among the diagnostic indicators of IM, the ROC/AUC for a villous pattern was high, at 0.77–0.80, except by the conventional method for the gastric body, suggesting that a villous pattern is an important diagnostic indicator of IM. The ROC/AUC values of a whitish mucosa and a rough mucosal surface by the conventional method for the gastric antrum and body and that of a whitish mucosa by the IC method for the gastric body were all approximately 0.75, suggesting that they are useful as diagnostic indicators of IM. As the rate of detection of atypical CV findings in the intermediate zone by the IC method was low, it was omitted. The ROC/AUC of an atypical CV finding detected by the conventional method in the gastric antrum and body was 0.7 or less, suggesting that this finding is not very useful as a diagnostic indicator of IM. The ROC/AUC values of patchy redness in the gastric antrum and body were all in the range of 0.5–0.6 by conventional and IC methods, making it inappropriate as a diagnostic indicator of IM.

When making an endoscopic diagnosis of IM based on the data of the present study, the conventional method should be carried out using a villous appearance, whitish mucosa, and rough mucosal surface in the gastric antrum and body as diagnostic indicators. In that case, the diagnostic performance in terms of ROC/AUC is more than 0.75. The addition of the areae gastricae pattern after 0.2% IC spraying will yield better diagnostic results.

The finding of a villous appearance and areae gastricae pattern in the gastric body and antrum by the IC method showed high diagnostic performance in endoscopic diagnosis of IM. In addition, the areae gastricae pattern is a finding that can only be obtained by the IC method. In this respect, the IC method is a useful diagnostic tool for IM and should be used in combination with the conventional method.

The present study had limitations. Prior to this study, each endoscopic finding was explained in order to standardize endoscopic findings and unify the accuracy of diagnosis among physicians participating in this study, whereas the assessment of endoscopic findings depended on each endoscopist.

In conclusion, conventional and IC methods yielded favorable results in the endoscopic diagnosis of intestinal metaplasia of the gastric mucosa.

ACKNOWLEDGMENT

THE PRESENT STUDY was supported by a grant from the Japanese Foundation for Research and Promotion of Endoscopy.

CONFLICT OF INTERESTS

AUTHORS DECLARE NO conflict of interests for this article.

REFERENCES

1 Magnus HA. Observations on the presence of intestinal epithelium in the gastric mucosa. *J. Pathol. Bacteriol.* 1937; **44**: 389–98.

2 IARC Working Group on the Evaluation of Carcinogenic Risks to Humans. Helicobacter pylori. In: IARC Working Group (ed.). *Schistosomes, Liverflukes, and Helicobacter pylori: Views and Expert Opinions of An IARC Working Group on the Evaluation of Carcinogenic Risks to Humans.* Lyon: IARC, 1994; 177–240.

3 Uemura N, Okamoto S, Yamamoto S *et al.* Helicobacter pylori infection and the development of gastric cancer. *N. Engl. J. Med.* 2001; **345**: 784–9.

4 Fukase K, Kato M, Kikuchi S *et al.* Effect of eradication of Helicobacter pylori on incidence of metachronous gastric carcinoma after endoscopic resection of early gastric cancer: An open-label, randomised controlled trial. *Lancet* 2008; **372**: 392–7. Original text.

5 Suzuki H, Iwasaki E, Hibi T. Helicobacter pylori and gastric cancer. *Gastric Cancer* 2009; **12**: 79–87.

6 Mutoh H, Sakurai S, Satoh K *et al.* Development of gastric carcinoma from intestinal metaplasia in Cdx2-transgenic mice. *Cancer Res.* 2004; **64**: 7740–7.

7 Magari H, Shimizu Y, Inada K *et al.* Inhibitory effect of etodolac, a selective cyclooxygenase-2 inhibitor, on stomach carcinogenesis in Helicobacter pylori-infected Mongolian gerbils. *Biochem. Biophys. Res. Commun.* 2005; **334**: 606–12.

8 Shiotani A, Iishi H, Uedo N *et al.* Histologic and serum risk markers for noncardia early gastric cancer. *Int. J. Cancer* 2005; **115**: 463–9.

9 Ushijima T, Nakajima T, Maekita T. DNA methylation as a marker for the past and future. *J. Gastroenterol.* 2006; **41**: 401–7.

10 Yang HB, Cheng HC, Sheu BS, Hung KH, Liou MF, Wu JJ. Chronic celecoxib users more often show regression of gastric intestinal metaplasia after Helicobacter pylori eradication. *Aliment. Pharmacol. Ther.* 2007; **25**: 455–61.

11 Capelle LG, de Vries AC, Haringsma J *et al.* The staging of gastritis with the OLGA system by using intestinal metaplasia as an accurate alternative for atrophic gastritis. *Gastrointest. Endosc.* 2010; **71**: 1150–8.

12 Niwa T, Tsukamoto T, Toyoda T *et al.* Inflammatory processes triggered by Helicobacter pylori infection cause aberrant DNA methylation in gastric epithelial cells. *Cancer Res.* 2010; **70**: 1430–40.

13 Nakajima T, Enomoto S, Yamashita S *et al.* Persistence of a component of DNA methylation in gastric mucosae after Helicobacter pylori eradication. *J. Gastroenterol.* 2010; **45**: 37–44.

14 Takemoto T. Endoscopic diagnosis of chronic gastritis. *Diagnosis and Treatment* 1966; **54**: 1274–85 (in Japanese).

15 Yokoyama I. Proceedings of 3rd Asian Pacific Congress of Gastroenterology, 2: Melbourne, 1968; 230.

16 Ida K, Hashimoto Y, Kawai K. In vivo staining of gastric mucosa: Its application to endoscopic diagnosis of intestinal metaplasia. *Endoscopy* 1975; **7**: 18–24.

17 Fennerty MB, Sampliner RE, McGee DL, Hixson LJ, Garewal HS. Intestinal metaplasia of the stomach: Identification by a selective mucosal staining technique. *Gastrointest. Endosc.* 1992; **38**: 696–8.

18 Kohli Y, Hattori S, Kodama T, Kawai K. Endoscopic diagnosis of intestinal metaplasia in asymptomatic (control) volunteers. *J. Gastroenterol.* 1979; **14**: 14–8.

19 Uedo N, Ishihara R, Iishi H *et al.* A new method of diagnosing gastric intestinal metaplasia: Narrow-band imaging with magnifying endoscopy. *Endoscopy* 2006; **38**: 819–24.

20 Ida K, Kohli Y, Shimamoto K, Hashimoto Y, Kawai K. Endoscopical findings of fundic and pyloric gland area using dye scattering method. *Endoscopy* 1973; **5**: 21–6.

21 Ida K, Tada M. *Chromoscopy. Special Method and Techniques in Gastroenterologic Endoscopy.* Philadelphia, PA: W.B. Saunders, 1987; 203–20.

22 Dixon MF, Genta RM, Yardley JH, Correa P. Classification and grading of gastritis. The updated Sydney System. International Workshop on the Histopathology of Gastritis, Houston 1994. *Am. J. Surg. Pathol.* 1996; **20**: 1161–81.

23 Kaminishi M, Yamaguchi H, Nomura S *et al.* Endoscopic classification of chronic gastritis based on a pilot study by the Research Society for Gastritis. *Dig. Endosc.* 2002; **14**: 138–51.

24 Kawai K, Sasaki Z, Misaki F, Ida K, Kubota Y. Endoscopic diagnosis of intestinal metaplasia of the stomach and its evaluation as a precancerous lesion. *Front. Gastrointest. Res.* 1979; **5**: 140–8.

Eur Spine J
DOI 10.1007/s00586-013-2686-8

ORIGINAL ARTICLE

Percutaneous vertebroplasty for osteoporotic vertebral compression fracture with intravertebral cleft associated with delayed neurologic deficit

Toshio Nakamae · Yoshinori Fujimoto · Kiyotaka Yamada · Haruhiko Takata · Takuro Shimbo · Yasuyuki Tsuchida

Received: 28 June 2012 / Revised: 24 November 2012 / Accepted: 25 January 2013

Abstract
Introduction The number of cases of osteoporotic vertebral compression fracture (OVCF) with intravertebral cleft (IVC) with delayed neurologic deficit (DND) is increasing as the population ages. However, the cause of DND is poorly understood, and no definitive treatment of the disease has been established. The purpose of this study was to clarify the radiographic parameters contributing to the occurrence of DND, and to evaluate the efficacy and safety of percutaneous vertebroplasty for this pathology.
Methods Percutaneous vertebroplasty was prospectively performed for 244 patients with OVCF with IVC; 30 had DND and 214 did not. Radiographic parameters of local kyphotic angle, percent spinal canal compromise and intravertebral instability were investigated for correlations to DND. Procedural outcomes were evaluated using visual analog scale (VAS), Oswestry Disability Index (ODI), and modified Frankel grades.
Results Before vertebroplasty, no substantial difference in local kyphotic angle was seen between OVCF with IVC with and without DND, but percent spinal canal compromise and intravertebral instability were greater in OVCF with IVC with DND ($P < 0.001$). After vertebroplasty, 25 of 30 cases (84 %) of OVCF with IVC with DND achieved clinically meaningful improvement (CMI), but 5 (17 %) did not. Patients with CMI showed substantial improvements in intravertebral instability ($P < 0.001$), and no change in local kyphotic angle or percent spinal canal compromise. In five patients without CMI, four showed an initial improvement, but subsequent vertebral fracture adjacent to the treated vertebra caused neurologic re-deterioration. One patient with percent spinal canal compromise 54.9 % and intravertebral instability 4° achieved no neurologic improvement following vertebroplasty. No serious complications or adverse events related to the procedure were encountered.
Conclusions Intravertebral instability is the dominant cause of DND. Percutaneous vertebroplasty appears effective and safe in the treatment of OVCF with IVC with DND. Patients with less intravertebral instability and severe spinal canal compromise could be candidates for conventional surgical treatment.

Keywords Percutaneous vertebroplasty · Osteoporotic vertebral fracture · Intravertebral cleft · Delayed neurologic deficit · Spine

Introduction

Osteoporotic vertebral compression fracture (OVCF) has been considered to show a benign natural history. However, rigorous follow-up studies have clarified that up to 30 % of OVCF does not respond adequately to standard conservative therapy [18, 22, 33]. Several reports have noted that the presence of Kümmell disease is associated with deteriorated prognosis for OVCF with intravertebral cleft (IVC). This disease could prolong back pain and predispose to vertebral collapse, which may result in

T. Nakamae (✉) · Y. Fujimoto · K. Yamada · H. Takata
Department of Orthopaedic Surgery,
JA Hiroshima General Hospital, Hiroshima, Japan
e-mail: toshinakamae623813@yahoo.co.jp

T. Shimbo
Department of Clinical Research and Informatics,
National Center for Global Health and Medicine,
Tokyo, Japan

Y. Tsuchida
Department of Radiology, JA Hiroshima General Hospital,
Hiroshima, Japan

Published online: 18 February 2013

delayed neurologic deficit (DND) [12, 14, 16, 17, 20, 21, 30]. The following factors have been suspected as causes of DND: (1) progression of kyphosis with vertebral collapse; (2) neural compression secondary to retropulsed bone fragments; and (3) intravertebral instability at the fracture site [1–3, 12, 13, 27, 32, 34]. The causes of DND with OVCF with IVC, however, remain poorly understood.

Surgical management has been performed for OVCF with IVC with DND. However, multiple medical comorbidities with advanced age and unreliable fixation in weakened osteoporotic bone have caused surgical treatments to result in significant morbidity and poor outcome [7, 9, 18]. On the other hand, the advent of vertebroplasty has marked a new era in the treatment of OVCF. This cement augmentation technique produces excellent outcomes in >85 % of patients treated [14]. However, percutaneous vertebroplasty for OVCF with IVC with DND may have been considered relatively contraindicated because of the possibility of neural complications induced by epidural cement leakage [4, 10, 14]. No definitive treatment of OVCF with IVC with DND has yet been established.

We have prospectively performed percutaneous vertebroplasty for OVCF with IVC with and without DND. The objectives of the current study were to clarify the radiographic parameters contributing to the occurrence of DND, and to evaluate the efficacy and safety of percutaneous vertebroplasty performed for OVCF with IVC with DND.

Materials and methods

Patients

A total of 321 consecutive patients with OVCF with IVC underwent percutaneous vertebroplasty at a tertiary referral center, JA Hiroshima General Hospital. For simple analysis of clinical data, 77 patients treated with vertebroplasty at more than a single level were excluded and the remaining 244 patients with single-level OVCF with IVC were enrolled in this study. The study protocol was approved by the ethics committee of our hospital, and written informed consent for this study design was obtained from all patients.

Radiographic diagnosis of OVCF with IVC

OVCF with IVC was radiographically diagnosed based on a positive finding of an intravertebral cleft described as an intravertebral transverse, linear radiolucent shadow on plain radiogram and/or CT, as a hypointense area on T2-weighted MR imaging similar to the signal intensity of gas, as a linear well-demarcated focus of T2 prolongation similar to the signal intensity of adjacent cerebrospinal fluid, and as a cleft-shaped non-contrast area within the vertebral body on fat-suppressed contrast-enhanced MR imaging, respectively (Fig. 1).

Clinical diagnosis of DND

Delayed neurologic deficit was clinically diagnosed based on the following criteria: (1) neurologically intact immediately after OVCF; (2) sensory and/or motor involvement appearing in an insidious and tardy process with progression of vertebral collapse; and (3) intractable pain of lower extremities in a sitting and/or standing position with improvement on lying down (*postural leg pain*) [5, 13, 25].

Inclusion and exclusion criteria

Selection criteria of percutaneous vertebroplasty for OVCF with IVC were: (1) sufficient back pain ≥4 (current rating

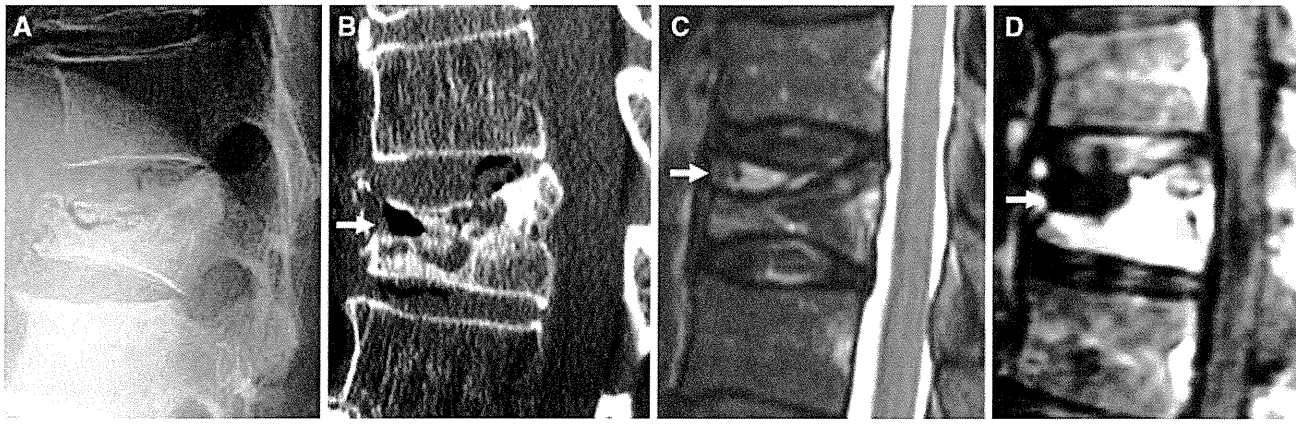

Fig. 1 The following sequence of images illustrates a patient with osteoporotic vertebral compression fracture with intravertebral cleft. **a** The fracture compresses through the intravertebral cleft beneath the superior endplate, demonstrating the maximal degree of height loss on lateral radiography with the patient in a sitting position. **b** The fracture plane gaps open because the patient is undergoing reformatted CT in a supine position (*arrow*). **c** Sagittal T2-weighed MR image demonstrating an area of hyperintensity within a region of hypointensity (*arrow*). **d** Sagittal fat-suppressed contrast-enhanced MR image revealing an intravertebral cleft as a non-contrast area (*arrow*)

for pain intensity on a scale from 0 to 10) refractory to standard medical treatment that consisted of bed rest, analgesics, and/or external back bracing for at least 3 months; and (2) radiographic OVCF with IVC with the presence of point tenderness on manual palpation. Exclusion criteria included: (1) spinal cancer, active infection, or uncorrectable bleeding diatheses; (2) inability to provide informed consent; and (3) a likelihood of noncompliance with direct follow-up.

Vertebroplasty technique

Experienced spine surgeons performed all procedures. After general anesthesia, patients were carefully positioned in a prone position with extended posture on a radiolucent four-poster spinal frame (Allen spinal system; Allen Medical Systems, Acton, MA). Next, 14-gauge bone needles (Ossiris; Hakko, Nagano, Japan) were inserted into an intravertebral cleft through a bilateral transpedicular approach with direct biplane observation using a couple of fluoroscopes (OEC 9900 Elite; GE Healthcare). The intravertebral cleft was a confluent reservoir and specifically targeted for polymethylmethacrylate (PMMA) (Osteobond; Zimmer, Warsaw, IN) injection. Before PMMA injection, cavitygram of the IVC was performed using nonionic contrast agent (Omnipaque 300; Nycomed, Princeton, NJ) to exclude needle placement within the basivertebral venous complex [6], and measured the capacity of the IVC. Persistent opacification could obscure visualization of the PMMA. The residual contrast material was washed out with normal saline to clear the IVC adequately to visualize PMMA. Barium-opacified PMMA of the same volume as the capacity of the IVC was gently injected using 2-ml syringes. PMMA was injected from the one-sided needle with low pressure and filled the IVC. PMMA assumed the shape of the IVC without evidence of extravasation into surrounding bone marrow space, paravertebral soft tissues or epidural space. The procedure was terminated when the cleft was filled with PMMA. On the next day after vertebroplasty, CT was performed to determine whether extravertebral PMMA leakage had occurred. A radiologist and orthopedic surgeon not involved in the procedure reviewed CT images independently and reached a consensus for each case.

Radiographic assessment

The following three radiographic parameters were assessed: (1) local kyphotic angle, measured as the angle between the lower and upper endplates of the uninvolved vertebrae adjusted cephalic and caudal to the fractured vertebra on lateral radiography with the patient in a sitting position; (2) percent spinal canal compromise, calculated by dividing the area of intrusion by total spinal canal area multiplied by 100; and (3) intravertebral instability of the affected vertebra, measured as the difference between local kyphotic angle on lateral radiography with the patient in a sitting position and that on sagittal reconstructed CT in a supine position (Fig. 2).

Outcome measures

Back pain and postural leg pain were measured using the VAS score of 0 to 10, with 0 indicating no pain, and 10 indicating the maximum imaginable pain [28]. Physical disability was measured on the ODI on a scale of 0 to 100 %, with higher scores indicating greater disability [8]. To measure various neurological symptoms at thoracolumbar junction, we used a modification of the Frankel neurologic grading system where ''A'' designated complete absence of motor and sensory function, and ''E2'' being the least neurologic impairment. We used the modified Frankel neurologic grading system because this system specifically focuses on the thoracolumbar neurologic functional impairment. For the quantitative analysis, we added a numeric numbering system to represent neurologic function on a scale of 1–7, with seven being complete deficit and one being the least affected (Table 1) [36]. Improvement rate was calculated using the following formula: (baseline score − postoperative score)/baseline score × 100 %. Clinically meaningful improvement (CMI) was defined as an improvement rate ≥30 % from baseline [24].

Patients were followed directly and periodically after vertebroplasty. In patients who died or could not return to our hospital, the latest complete neurologic examination and radiographs were used for evaluation. Orthopedic surgeons not involved in treatment performed the follow-up and clinical examinations to assess neurologic recovery and functional status. The questionnaire of the VAS score and ODI was self-administered to avoid interviewer bias.

Statistical analysis

To clarify causes of DND, we compared radiographic parameters between the DND group and the control group consisting of non-DND patients. This study was designed to have the number of patients in the DND group and the control group at a ratio of 1:2. The matching criteria were age in years (based on decade), sex and spinal level of OVCF with IVC. Plain radiogram and CT were mixed and observers were blinded to the clinical status of patients. Variability of intraobserver measurement was within 3 % for the entire study. In addition, pre- and post-procedural radiographic parameters were compared in patients with

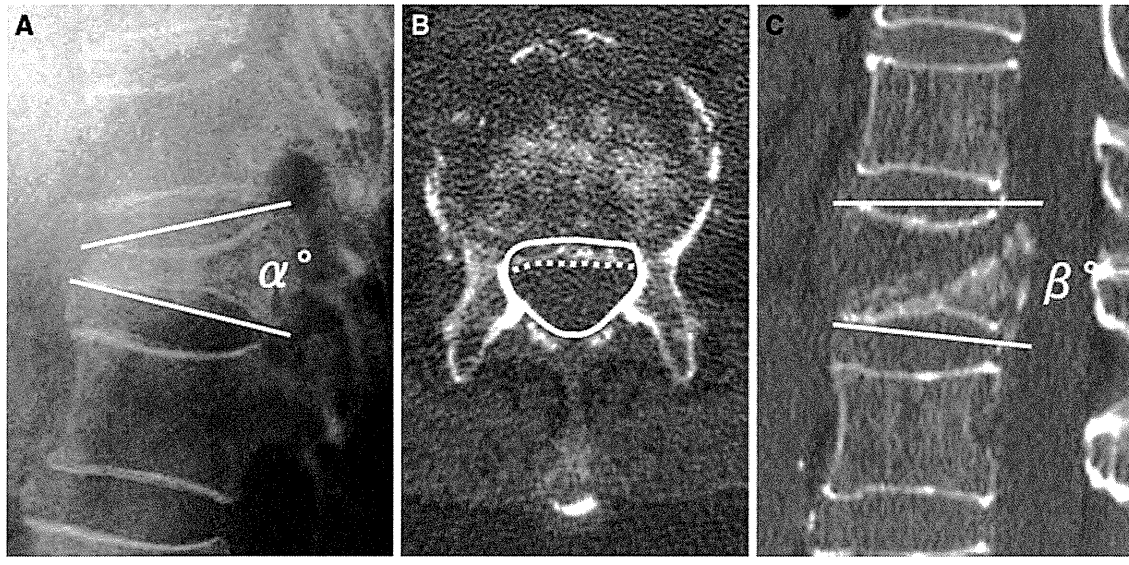

Fig. 2 Three radiographic parameters demonstrating **a** "local kyphotic angle" (α°) measured using Cobb's method with the patient in a sitting position and **b** "percent spinal canal compromise" calculated by dividing the area of intrusion by the total spinal canal area multiplied by 100. The total canal area is outlined by the *solid line*; the area of the retropulsed vertebral wall is demarcated by the *dotted line*. Areas of the spinal canal and retropulsed posterior wall are calculated from the total number of pixels per cross-sectional area (pixel/mm^2). **a**, **c** "Intravertebral instability", defined as the difference between local kyphotic angle on lateral radiography with the patient in a sitting position (α°) and that on a sagittal reformatted CT scan in a supine position (β°); α°–β°

Table 1 Numeric neurologic functional grades

7-A	Complete motor and sensory loss
6-B	Sensation preserved. No voluntary motor function
5-C	Motor function less than fair grade (nonfunctional for any useful purposes)
4-D1	Preserved motor at lowest functional grade; MMT 3+/5+
3-D2	Preserved motor at midfunctional grade; MMT 3+ to 4+/5+
2-E1	Preserved motor ad high functional grade; MMT 4+ to 5+/5+
1-E2	Motor and sensory function normal. May still have abnormal reflexes
0-F	Normal

Modified Frankel neurologic functional grades are represented by the alphabet letter; a numeric designation precedes the letter

DND who achieved CMI. To evaluate the efficacy and safety of vertebroplasty, procedural outcomes and procedure-related complications were compared between patients with and without DND.

Clinical characteristics and radiographic parameters were analyzed using the Mann–Whitney *U* test or Chi-square test. Associations between radiographic parameters and DND were analyzed using multivariate logistic-regression models. Procedural outcomes were analyzed using the Wilcoxon signed-ranks test, Mann–Whitney *U* test, and/or the Bonferroni–Dunn post hoc test. Procedure-related complications were analyzed with the Mann–Whitney *U* test, Chi-square test, or Fisher's exact test. Statistical significance was defined at the level of $p < 0.05$ for a two-sided hypothesis. Mean data are presented ± standard deviation. Analyses were performed using SPSS version 16.0 (SPSS, Chicago, IL).

Results

Baseline characteristics of the 244 patients

Of the 244 patients, 30 had DND and 214 did not (Table 2). OVCF with IVC clustered at the thoracolumbar junction (T11–L2), seen in 26 of 30 (87 %) OVCF with IVC cases with DND and 177 of 214 (83 %) OVCF with IVC cases without DND. No significant differences between groups were seen in age, sex, spinal level of OVCF with IVC, or duration from OVCF to vertebroplasty.

Patients with OVCF with IVC were unable to perform activities of daily living because of severe back pain. Physical ability was more greatly disturbed in OVCF with IVC with DND. Among 12 patients with a numeric neurologic functional grade of 5-C, six patients with T12 OVCF with IVC showed bilateral drop-foot without leg

Table 2 Baseline characteristics of the 244 patients

Characteristic parameters	DND group ($n = 30$)	Non-DND group ($n = 214$)
Age (year)	77.5 ± 8.2	77.0 ± 7.0
Female sex—no. (%)	24 (80)	146 (68)
Spinal level of OVFC with IVC—no. (%)		
T7–T10	2 (7)	12 (6)
T11	1 (3)	15 (7)
T12	11 (37)	69 (32)
L1	9 (30)	72 (34)
L2	5 (17)	21 (10)
L3–L5	2 (7)	25 (12)
Duration from OVFC to PVP (week)	19.2 ± 11.2	28.7 ± 36.4
Duration from OVFC to DND (week)	9.1 ± 9.0	–
VAS score for back pain	8.1 ± 3.9	8.6 ± 1.4
ODI†	73.9 ± 13.4 %	51.1 ± 21.9
Numeric neurologic functional grade—no. (spine level of OVFC with IVC—no.)		
5-C	12 (T10—2, T12—7, L1—1, L2—2) six patients with T12 OVFC with IVC had bilateral drop-foot	–
4-D	2 (T12—2)	–
3-D2	4 (L1—2, L3—2)	–
2-E1	12 (T11—1, T12—2, L1—6, L2—3) all patients had postural leg pain, VAS: 8.2 ± 1.8	–
0-F	–	214

Plus-minus values are mean ± SD

DND delayed neurologic deficit, *IVC* intravertebral deft, *PVP* percutaneous vertebroplasty, *VAS* visual analog scale, *ODI* Oswestry disability index

† $P < 0.001$ for the comparison between the two groups

Table 3 Radiographic parameters before vertebroplasty, the DND group vs. the control group

Radiographic parameters	DND group ($n = 30$)	Control group ($n = 60$)	Odds ratio
Local kyphotic angle (°)	17.0 ± 8.8	15.6 ± 7.7	[0.94; 95 % [CI] 0.88–1.04; $P = 0.31$]
Percent spinal canal compromise (%)†	35.4 ± 13.1	23.1 ± 11.1	[1.10; 95 % [CI] 1.05–1.17; $P < 0.001$]
Intravertebral instability (°)†	10.6 ± 5.9	5.3 ± 3.3	[1.43; 95 % [CI] 1.18–1.73; $P < 0.001$]

Plus-minus values are mean ± SD. Logistic regression analysis with multivariate models shows independence and specific correlation between the radiographic parameters and DND [odds ratio; 95 % confidence interval (CI); *P* value]

DND delayed neurologic deficit

† $P < 0.001$ for the comparison by the Mann–whitney *U* test between the two groups

pain. All 12 patients with grade 2-E1 had severe postural leg pain involving bilateral thighs, which deteriorated in a sitting and/or standing position and compelled the patients to remain lying down or bedridden.

Radiographic assessment before vertebroplasty

Mean local kyphotic angle, percent spinal canal compromise, and intravertebral instability were 17.0 ± 8.8°, 35.4 ± 13.1 %, and 10.6 ± 5.9° in the DND group, and 15.6 ± 7.7°, 23.1 ± 11.1 %, and 5.3 ± 3.3° in the control group, respectively. No significant difference in local kyphotic angle was evident between groups. However, percent spinal canal compromise and intravertebral instability were greater in the DND group than in the control group ($P < 0.001$). Logistic regression analysis with multivariate models showed that local kyphotic angle had no substantial correlation to DND, while percent spinal canal compromise and intravertebral instability were associated with DND (Table 3).

Outcomes of vertebroplasty

All 30 patients with DND (100 %) and all 214 patients without DND (100 %) were directly followed at 1 and

6 months; follow-up was maintained for 25 (83.3 %) and 176 (82.2 %) at 12 months, and 25 (83.3 %) and 162 (75.7 %) at 24 months after vertebroplasty, and the duration of follow-up was 18.6 ± 12.6 and 28.5 ± 10.1 months, respectively. General health problems associated with advanced age made it difficult for patients to attend our clinical examination.

CMI was achieved in 25 patients with DND (83.3 %) and 161 without DND (75.2 %). VAS scores for back pain and postural leg pain as well as ODI were meaningfully improved immediately after vertebroplasty. Numeric neurologic functional grades gradually improved (Fig. 3). No significant differences in improvement rate of VAS score and ODI were seen between groups during the period of direct follow-up. Bilateral drop-foot in six patients recovered with manual muscle testing scores for tibialis anterior muscles from 1.7 ± 0.5 before vertebroplasty to 2.5 ± 1.3 at 1 month ($P = 0.32$), and 4.0 ± 1.4 at 3 months ($P = 0.024$) after the intervention.

Five patients with DND (17 %) and 53 without DND (25 %) failed to achieve CMI. Four patients with DND and 53 without DND showed an initial improvement following vertebroplasty, but subsequent vertebral fracture adjacent to the treated vertebra resulted in deteriorated outcomes. No significant difference in incidence of vertebral fracture adjacent to the augmented vertebra was seen between groups ($P = 0.57$). Only 1 patient with DND had percent spinal canal compromise of 54.9 % and intravertebral instability of 2°, with no neurologic improvement following vertebroplasty.

Radiographic parameters in patients with DND who achieved CMI

Table 4 shows pre- and post-procedural radiographic parameters in the 25 patients with DND who achieved CMI. No substantial improvements were seen in local kyphotic angle or percent spinal canal compromise, but intravertebral instability was significantly improved after vertebroplasty ($P < 0.001$).

Procedure-related complications

The cement volume injected was 6.3 ± 2.7 ml (range, 1.8–12 ml) and 4.0 ± 2.6 ml (range, 0.5–12 ml) in cases of OVCF with IVC with and without DND, respectively, with a substantially larger volume in OVCF with IVC with DND ($P < 0.001$). No significant difference in incidence of cement leakage was seen between OVCF with IVC with DND (3 of 30, 10 %) and without DND (53 of 214, 24.8 %) ($P = 0.07$). Leakage occurred into the epidural veins (0 of 30), perivertebral soft tissue (0 of 30), intervertebral disc space (3 of 30, 10 %) and lung (0 of 30) in OVCF with IVC with DND and into the epidural veins (3 of 214, 1.4 %), perivertebral soft tissue (11 of 214, 5.1 %), intervertebral disc space (39 of 214, 18.2 %) and lung (0 of 214) in OVCF with IVC without DND (Table 5). No patients in the current study presented with neurologic deterioration related to epidural cement leakage, or with systemic complications such as cement embolism that could be attributed to the procedure itself.

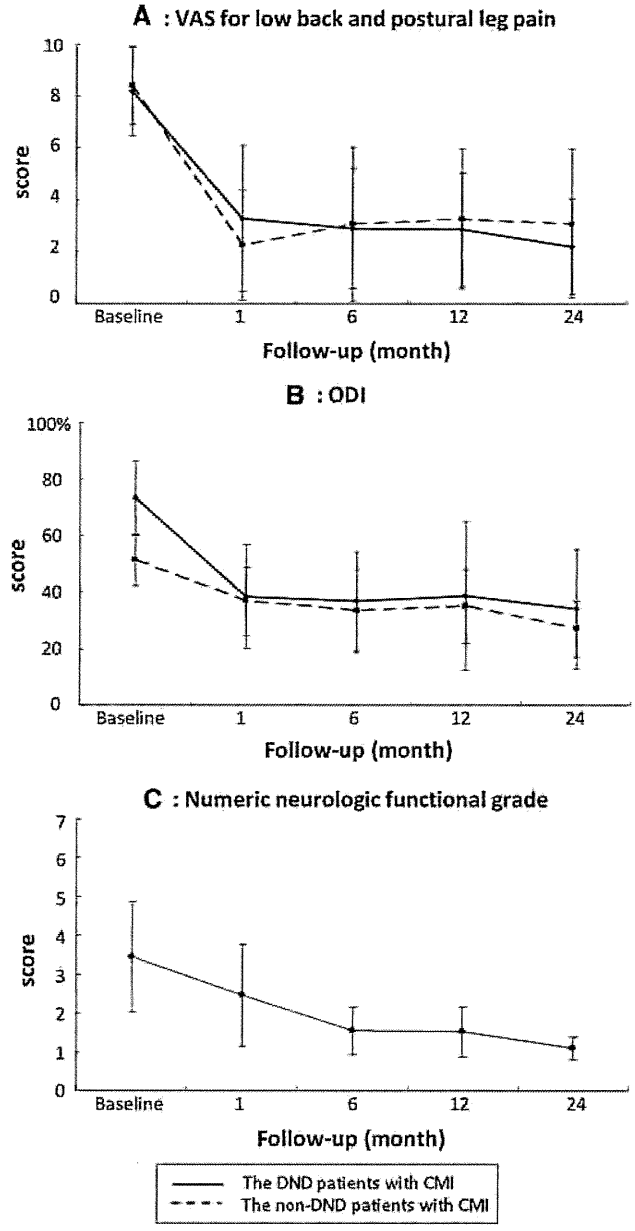

Fig. 3 Post-procedural scores of VAS, ODI, and numeric neurologic functional grade in patients with CMI. VAS score for low back pain (**a**) and ODI (**b**) were improved immediately after vertebroplasty ($P < 0.001$). Numeric neurologic functional grade (**c**) gradually improved after the intervention (1 month: $P = 0.005$; 6–24 months: $P < 0.001$) for comparison with baseline scores. Results are expressed as mean ± standard deviation (SD). *VAS* visual analog scale, *DND* delayed neurologic deficit, *CMI* clinically meaningful improvement, *ODI* Oswestry disability index